TWELFTH EUROPEAN ROTORCRAFT FORUM

Paper No. 28

COMPUTATION OF THE FLOW FIELDS OF PROPELLERS AND HOVERING ROTORS USING EULER EQUATIONS

N. Kroll

DFVLR, Institute for Design Aerodynamics
Braunschweig, F.R. Germany

September 22 - 25, 1986

Garmisch-Partenkirchen
Federal Republic of Germany

Deutsche Gesellschaft für Luft- und Raumfahrt e. V. (DGLR)
Godesberger Allee 70, D-5300 Bonn 2, F.R.G.

COMPUTATION OF THE FLOW FIELDS OF PROPELLERS AND HOVERING ROTORS USING EULER EQUATIONS

N. Kroll
DFVLR, Institute for Design Aerodynamics
Braunschweig, F.R. Germany

ABSTRACT

A numerical procedure for the calculation of the flow fields of propellers and hovering rotors is described. The method solves the three-dimensional Euler equations which are formulated in terms of the flow variables in a blade-attached cartesian reference frame. The solution algorithm is based on the finite volume method originated by Jameson et al. using explicit Runge-Kutta time-stepping schemes. Calculations are presented for subsonic and transonic flows around a two-bladed propeller and a two-bladed model helicopter rotor in hover. The theoretical results show good agreement with the experimental data.

1. INTRODUCTION

During the last few years a wide variety of numerical methods for simulating the complex flow fields of rotary wing configurations has been developed. An overview of the methods for propeller and rotorcraft applications is given in the papers [1] and [2] respectively.

Most of the algorithms predicting inviscid flows are based on the potential flow assumption. At present, linear methods such as lifting line or lifting surface techniques are routinely used. However, these methods are limited to linearized theories for compressible flows. In order to treat transonic flows associated with high speed advancing propellers or rotors, several numerical procedures based on the small-disturbance as well as the full potential equation have been developed. The main limitation of the potential flow model is that the roll-up of the vortex wake attached to the rotary blade and the convection of the tip vortex past the blade are not taken into account. Since the flow field of a lifting rotary wing is mainly determined by the wake system, a suitable wake modeling has to be incorporated into potential flow methods.

Recent advances in computer performance and computational techniques have made it possible to solve the three-dimensional Euler equations for a wide variety of aerodynamic applications. The Euler equations describe the inviscid transonic flow correctly regardless of the strength of the appearing shocks. Unlike the potential flow model the Euler equations allow entropy rise through shock waves while mass, momentum and energy are conserved. This leads to an accurate prediction of the location and strength of the shock. The most important feature of the Euler equation model for rotary wing applications is that vortical solutions are admitted.

Since vorticity is captured and convected the complex wake geometry of rotary wing flows does not have to be prescribed but is a part of the solution. Due to the high computational expense the numerical solution of the Euler equations for rotary wing configurations at present are primarily limited to steady flows such as the flow fields of propellers in axial flight and hovering rotors. Several papers have addressed the prediction of the flow fields of high speed propellers. Bober et al. [3] developed a three-dimensional Euler code for a multibladed propeller and axisymmetric nacelle combination. His finite difference scheme is based on the Beam and Warming code and solves the Euler equations which are formulated in a cylindrical coordinate system. Holmes and Tong [4] applied the finite volume method of Jameson to turbine blade rows and propellers using cartesian coordinates. Recently Calestina et al. [5] presented results of the numerical simulation of the time-averaged inviscid flow field through a counterrotating propeller.

Solutions of the Euler equations for hovering rotors are presented in [6,7] . In order to eliminate numerical diffusion of the rolled-up wake vorticity due to trunction error and artificial viscosity, Roberts and Murman [6] developed a computational procedure in which the velocity field is decomposed into two parts. The total velocity is the sum of the induced velocity of the vortex wake which is known from a free wake analysis and the unknown velocity field of the rotor blade computed by the solution of the Euler equations. Calculations on a relatively coarse grid show that the results were improved by adding the vortex wake. A similar method was also outlined by Sankar et al. [7]. Recently Wake et al. [8] have presented results for unsteady three-dimensional transonic flows around nonlifting rotor blades.

The present paper describes an extension of the DFVLR Euler code for nonrotating wings [9] which allows calculation of flow fields of propeller and hovering rotor blades. A blade-attached cartesian coordinate system is used to formulate the conservation equations in terms of the absolute flow variables as outlined in [4]. The solution procedure is based on the finite volume scheme of Jameson et al. [10]. Unlike the methods presented in [6,7] no vortex wake model is used in the present work. Results are presented for a two-bladed propeller and a two-bladed model rotor in hover.

2. GOVERNING EQUATIONS

In a blade-attached coordinate system rotating with a constant angular velocity Ω , the flow field of a propeller in axial flight as well as that of a hovering rotor can be treated as steady. In this reference frame the Euler equations can be formulated in terms of either relative or absolute flow variables. The results presented in this paper were obtained using the formulation with absolute flow variables.

With the rotation axis showing in x-direction, the Euler equations in cartesian coordinates are written in integral form as

$$\frac{\partial}{\partial t} \iiint_{\sigma} \vec{W}\, d\sigma + \iint_{\partial\sigma} (\bar{\bar{F}} - \bar{\bar{G}})\cdot\vec{n}\, ds + \iiint_{\sigma} \vec{S}\, d\sigma = 0 \qquad (1)$$

where σ denotes a fixed region in the blade-attached coordinate system with boundary $\partial\sigma$ and outer normal $\vec{n}$. $\vec{W}$ represents the conserved vector of absolute flow variables, $\bar{\bar{F}} - \bar{\bar{G}}$ the corresponding flux tensor and $\vec{S}$ is a source term. These quantities are given by

$$\vec{W} = \begin{bmatrix} \rho \\ \rho u \\ \rho v \\ \rho w \\ \rho E \end{bmatrix}, \bar{\bar{F}} = \begin{bmatrix} \rho\vec{q} \\ \rho u\vec{q} + p\vec{i}_x \\ \rho v\vec{q} + p\vec{i}_y \\ \rho w\vec{q} + p\vec{i}_z \\ \rho H\vec{q} \end{bmatrix}, \bar{\bar{G}} = \begin{bmatrix} \rho\vec{\omega}\times\vec{r} \\ \rho u\vec{\omega}\times\vec{r} \\ \rho v\vec{\omega}\times\vec{r} \\ \rho w\vec{\omega}\times\vec{r} \\ (\rho H - p)\vec{\omega}\times\vec{r} \end{bmatrix}, \vec{S} = \begin{bmatrix} 0 \\ 0 \\ -\rho\Omega w \\ \rho\Omega v \\ 0 \end{bmatrix}$$

where ρ is the density, p is the pressure, E is the total energy, H is the total enthalpy, $\vec{q}=(u,v,w)$ is the absolute velocity, $\vec{r}$ is the position vector, $\vec{\omega}=(\Omega,0,0)$ is the angular velocity and $\vec{i}_x,\vec{i}_y,\vec{i}_z$ denote the unit vectors of the cartesian coordinate system. The pressure is obtained by

$$p = \rho(\gamma-1)\left(E - \frac{1}{2}(u^2+v^2+w^2)\right) \qquad (2)$$

where γ is the ratio of specific heats.

The relative velocity $\hat{\vec{q}}$ is given by

$$\hat{\vec{q}} = \vec{q} - \vec{\omega}\times\vec{r} \qquad (3)$$

$\bar{\bar{G}}$ and $\vec{S}$ in equation (1) represent the terms due to the rotation of the coordinate system. For $\Omega=0$ system (1) reduces to the Euler equations for a nonrotating reference frame.

At solid surface normal velocity has to be zero, that is

$$(\vec{q} - \vec{\omega}\times\vec{r})\cdot\vec{n} = 0 \qquad (4)$$

where $\vec{n}$ denotes the unit vector normal to the surface. Equation (1) with absolute flow variables leads to a uniform rather than a rotating far field. The flow at the far field is assumed to be undisturbed and free stream conditions are imposed.

In this paper only a two-bladed propeller and hovering rotor are considered. Because of periodicity only the flow around one blade has to be computed.

3. NUMERICAL PROCEDURE

The solution method is an extension of the block-structured 3-D Euler code for a nonrotating reference frame developed at DFVLR [9]. The procedure is based on the finite volume method using an explicit multistage time-stepping scheme originated by Jameson et al. [10]. In the following both grid generation and solution algorithm are briefly described with special emphasis on the discretization of terms which arise due to rotation of the coordinate system. Details of the basic scheme are given in Radespiel and Kroll [9].

3.1 Grid Generation

The body-fitted grids used in the present paper have been generated algebraically by the transfinite interpolation method described by Eriksson [11]. The grids around the propeller and rotor blades have O-O topologies (Fig. 1) which provides a good resolution at leading and trailing edges as well as at the tip of the blade.

In most cases a grid with a total of 96x20x36 cells has been used, 96 cells around the blade profile, 20 cells normal to the blade and 36 cells along the blade span. The outer boundary of the grid has been placed about 20 chords away from the surface (Fig. 2). For the hovering rotor case a finer grid with a total of 123x32x36 cells has been used.

Because of the strong twist of a propeller special care has to be taken in constructing the surface grid of the outer boundaries of the computational domain. In order to avoid intersections or excessively skewed cells the outer boundary has also been twisted, as indicated in Fig. 2.

For the propeller blade the details of the grid are shown in Fig. 3. The surface grid is given in Fig. 3a. The sectional grids for two spanwise sections and a view of a spanwise section are shown in Fig. 3b and 3c respectively.

3.2 Solution Algorithm

Semi-discretization of equation (1) decouples spatial and time discretization. Associating the discrete absolute flow quantities $\vec{W}_{i,j,k}$ with the cell centers the finite volume spatial discretization results in

$$\frac{d}{dt}(h_{i,j,k}\,\vec{W}_{i,j,k}) + \vec{Q}_{i,j,k} - \vec{D}_{i,j,k} + h_{i,j,k}\,\vec{S}_{i,j,k} = 0 \qquad (5)$$

where $h_{i,j,k}$ denotes the cell volume of hexahedral cells. $\vec{Q}_{i,j,k}$

is the approximation of the surface integral of equation (1) and represents the sum of the Euler fluxes for each cell. The surface integral is evaluated assuming the absolute flow variables to be constant on the cell faces. They are calculated as the average of the values $\vec{W}_{i,j,k}$ at the corresponding cell centers. Following the idea of Holmes and Tong [4] the volume flux

$$\iint_{\partial\sigma} (\vec{q} - \vec{\omega}\times\vec{r}) \cdot \vec{n} \, ds$$

of a cell face is split into a term involving the absolute velocity and a term involving only the rotational velocity. The integral of the volume flux due to the absolute velocity is approximated using the mid-point rule, whereas the integral of the volume flux due to the rotational velocity is determined purely by local geometrical quantities and can therefore be calculated exactly for each cell face using the Stokes theorem. Thus, no approximation is used to evaluate the terms involving the rotational velocity. This has been found to be essential in order to ensure that the freestream is a solution of the discrete equations of system (1) on a nonuniform grid. The source term $\vec{H}$ is taken to be volume-averaged and is located at the cell center.

In order to damp out high frequency oscillations and to avoid oscillations in the neighbourhood of shock waves, dissipative terms $\vec{D}_{i,j,k}$ [10] are added. The terms are formed by a blend of second and fourth differences of the absolute flow variables.

In the finite volume scheme the solid surface boundary condition results in the condition that all convective fluxes are zero at the wall. The only quantities which are required at the wall are the pressure and the volume flux velocity due to the rotation. The pressure is obtained by linear extrapolation from the interior and the rotational volume flux is known from the grid geometry. At the far field, freestream conditions are imposed. Furthermore, a periodic boundary condition is applied on the coordinate surface at the blade root.

To integrate the system (5) of ordinary differential equations in time, an explicit 5-stage Runge-Kutta time stepping scheme with only two evaluations of the dissipative terms has been used. The convergence to steady state is accelerated by local time-stepping, implicit residual averaging [12] and successive grid refinement. Furthermore, the technique of enthalpy damping [10] has been applied to the rothalpy $\hat{H}$ defined by

$$\hat{H} = H - \vec{q} \cdot (\vec{\omega}\times\vec{r}) \qquad (6)$$

since the rothalpy is constant in the case of a propeller in axial flight as well as that of a hovering rotor.

The code is structured to use an arbitrary number of blocks in the computational domain. It efficiently uses the CRAY-1S vector computer and allows calculations with a nearly unrestricted number of grid points on arbitrary grid topologies. The details

of the multiblock structure implemented in the program are found in Radespiel and Kroll [9].

4. RESULTS AND DISCUSSION

The basic 3-D Euler code has been extensively tested for non-rotating wings (see [9],[13]). In the present paper calculations have been performed for two rotary wing configurations, a two-bladed propeller and a two-bladed model rotor in hover.

4.1 NACA 10-(3)(066)-033 Propeller

In the early post-war years a series of wind tunnel tests on full scale propellers was carried out by NACA. The tests provide pressure distributions on the rotating blade at a number of radial stations. Results have been obtained for the two-blade ten ft. diameter NACA 10-(3)(066)-033 propeller [14]. The blade, incorporating NACA 16-series blade sections, has a rectangular planform. The geometry of the two-blade propeller is shown in Fig. 4. Computations have been performed for the transonic flow with free-stream Mach number $M_\infty = 0.56$ and advance ratio $J = 2.3$. Figure 4 shows the comparison of the calculated and measured pressure distribution at four different span sections. The theoretical results are in good agreement with the experiment. The differences may be due to the effect of the boundary layers along the surface which is not accounted for in the calculation.

4.2 Model Rotor in Hover

The second set of calculations for rotating systems was that of a model helicopter rotor in hover as tested by Caradonna and Tung [15]. The rotor blade incorporated constant NACA 0012 airfoil sections and is untwisted as well as untapered and has an aspect ratio of 6. Measurements were carried out for a wide range of collective pitch angles and tip Mach numbers including the transonic flow regime.

Calculations have been performed for a collective pitch setting $\theta = 8^o$ and tip Mach number $M_{tip} = 0.439$. In this case an O-O type grid with a total of 128x32x36 cells has been used. Fig. 5 shows the comparison of computed and experimental surface pressure coefficients at five different span sections. Note that for the calculations presented in this paper no wake model has been used. The theoretical and experimental data on both the upper and lower surfaces agree fairly well. At 68 and 80 percent span the computed pressure distributions show larger suction peaks at the leading edge than the experimental data. This may indicate that the used grid is not fine enough to calculate accurately the strong downwash which reduces the effective angle of attack of the blade sections. However, at 96 percent span the suction peak is underpredicted by the computation. A satisfactory reason for this has not yet been found. Due to the present grid generation technique

the planform and the thickness is locally modified at the blade tip by a smoothing procedure. Calculations, in which the beginning of the modification has been varied between 0.975 and 0.995 percent span, showed no significant effects on the pressure distribution at 0.96 percent span.

In order to show the influence of the grid fineness on the surface pressure coefficients the above results are compared with those obtained on a coarser grid with half of the cells in each coordinate direction (Fig. 6). Fig. 6 contains, in addition, the results of Roberts and Murman [6] which have been obtained by the solution of Euler equations using an additional wake model. Their calculation has been performed on a similarly coarse grid with a total of 64x14x16 cells. The present coarse grid results for the surface pressure coefficients are in close correspondence with their data. However, the present fine grid results show the best agreement with experimental data. In particular, the prediction of the suction peak at the leading edge and the pressure distribution on the lower surface are improved. The sectional lift coefficient is significantly reduced with grid refinement as shown in Fig. 7. The comparison with the experimental data indicates that a still finer grid is necessary to predict the flow field of a hovering rotor accurately. Therefore, implementation of the local grid refinement technique is planed. This provides an efficient and accurate solution of the three-dimensional Euler equations. The technique is already incorporated in the DFVLR Euler code for wings in translatory motion [16].

Computations have also been performed for transonic case with collective pitch angle $\theta = 8^{\circ}$ and tip Mach number 0.794. Again, the comparison of calculated and experimental surface pressure coefficients shows reasonable agreement (Fig. 8).

5. CONCLUSIONS

A numerical procedure for the prediction of the flow fields of propeller and hovering rotor blades has been described. It solves the Euler equations formulated in terms of the absolute flow variables in a blade-attached coordinate system. No additional vortex wake model has been used to simulate the flow.

Calculations for both subsonic and transonic flows around a two-bladed model rotor in hover as well as transonic flow around a two-bladed propeller have been presented. Algebraically generated grids having O-O topology have been used. The comparison of the calculated and experimental surface pressure coefficients shows good agreement. The grid has to be fine enough in order to resolve the effects of the tip vortex. Otherwise the sectional lift coefficient will be overpredicted.

ACKNOWLEDGEMENTS

The author would like to thank Dr. A. KUMAR from NAL Bangalore, India, who developed the grid generation code and some of the graphic programs used in this paper. Further acknowledgements are due to the colleagues Dr. R. RADESPIEL and C. ROSSOW for some intensive discussions.

REFERENCES

1. Ph. Poisson-Quinton — Technical Evaluation Report on the Fluid Dynamics Panel Symposium on Aerodynamics and Acoustics of Propellers. AGARD-AR-213 (1985).

2. J.J. Philippe, P. Roesch, A.M. Dequin, A. Cler — A Survey of Recent Development in Helicopter Aerodynamics. AGARD-LS-139 (1985).

3. L.J. Bober, D.S. Chaussee, P. Kutler — Prediction of High Speed Propeller Flow Using a Three-Dimensional Euler Analysis. AIAA Paper 83-0188 (1983).

4. D.G. Holmes, S.S. Tong — A Three-Dimensional Euler Solver for Turbomachinery Blade Rows. ASME Journal of Engineering for Gas Turbines and Power, (1985) Vol. 107, pp. 258-264.

5. M.L. Celestina, R.A. Mulac, J.J. Adamczyk — A Numerical Simulation of the Inviscid Flow Through a Counterrotating Propeller. Presented at ASME Gas Turbine Conference, June 8-12 (1986).

6. T.W. Roberts, E.M. Murman — Solution Method for a Hovering Helicopter Rotor Using the Euler Equations. AIAA Paper 85-0436 (1985).

7. N.L. Sankar, B.E. Wake, S.G. Lekoudis — Solution of the Unsteady Euler Equations for Fixed and Rotor Wing Configurations. AIAA Paper 85-0120 (1985).

8. B.E. Wake, N.L. Sankar, S.G. Lekoudis — Computation of Rotor Blade Flows Using the Euler Equations. Journal of Aircraft (1986), Vol. 23, pp. 582-588.

9. R. Radespiel N. Kroll — Progress in the Development of an Efficient Finite Volume Code for the Three-Dimensional Euler Equations. DFVLR-FB-85-31 (1985).

10. A. Jameson, W. Schmidt, E. Turkel — Numerical Solutions of the Euler Equations by Finite Volume Methods Using Runge-Kutta Time-Stepping Schemes. AIAA Paper 81-1259 (1981).

11. L.E. Eriksson — Generation of Boundary Confirming Grids Around Wing-Body Configurations Using Transfinite Interpolation. AIAA Journal (1982), Vol. 20, pp. 1313-1320.

12. A. Jameson, T.J. Baker — Solution of the Euler Equations for Complex Configurations. AIAA-Paper 83-1929 (1983).

13. G. Wichmann, R. Radespiel, S. Leicher — Vergleich von Lösungen der vollständigen Potentialgleichung und der Eulergleichungen für die Transsonische Umströmung des DFVLR-F4-Flügels. DGLR-Jahrbuch 1985.

14. J.D. Maynard, M.P. Murphy — Pressure Distributions on the Blade Sections of the NACA 10-(3)(066)-033 Propeller Under Operating Conditions. NACA-RM L9L12 (1950).

15. F.X. Caradonna, C. Tung — Experimental and Analytical Studies of a Model Helicopter Rotor in Hover. NASA TM 81232 (1981).

16. R. Radespiel — Efficient Solution of Three-Dimensional Euler Equations Using Embedded Grids. ICAS-86-1.3.3 (1986).

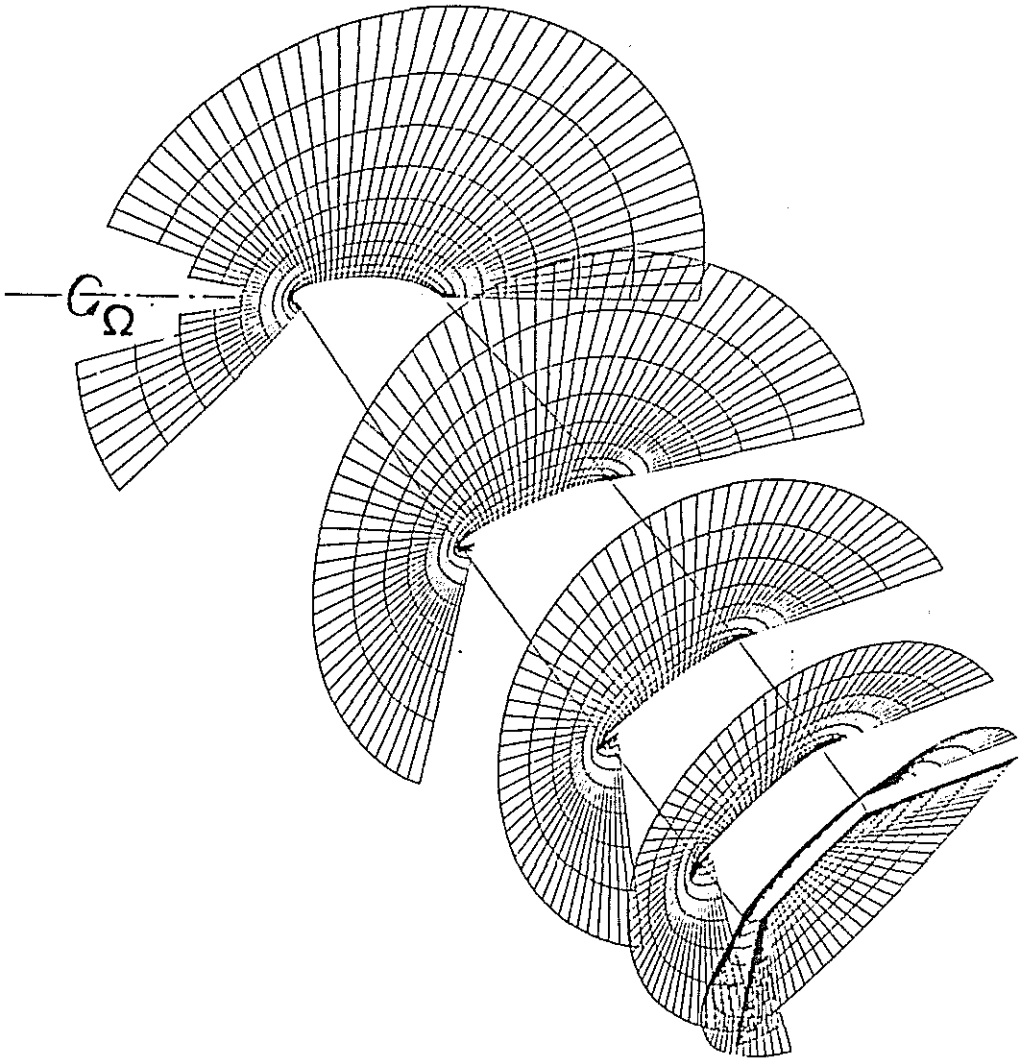

Fig. 1 O-O type grid for a propeller blade

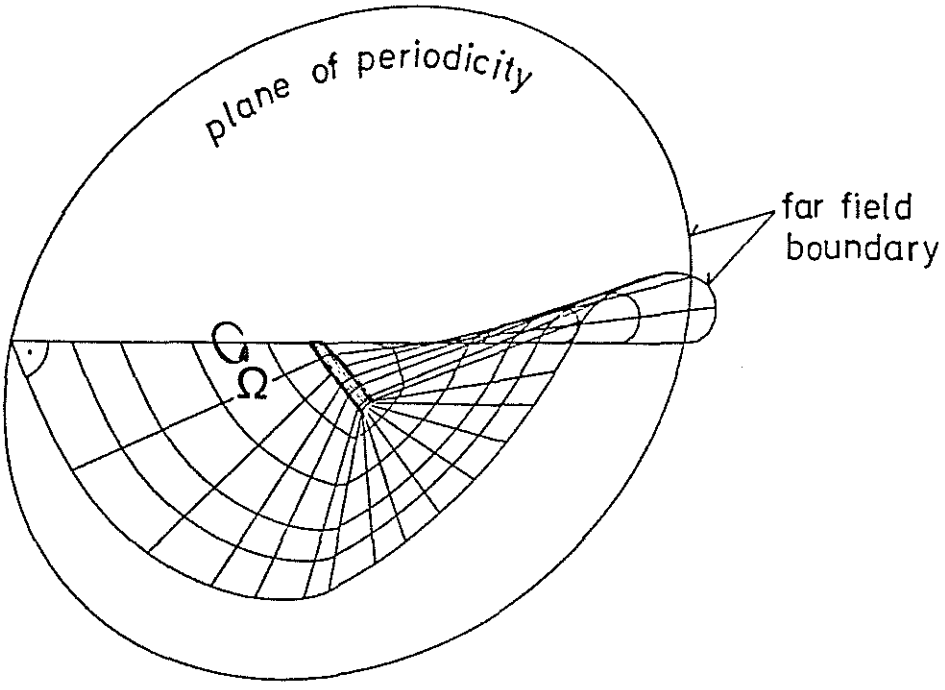

Fig. 2 Outer boundaries of the computational domain

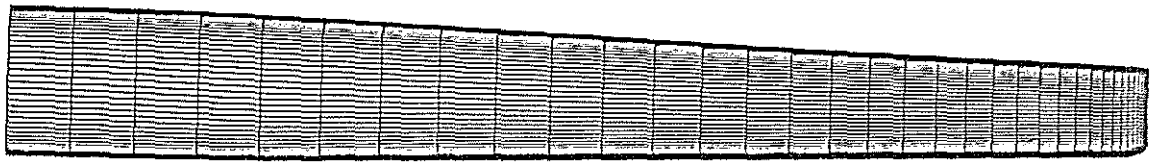

a) Blade surface grid

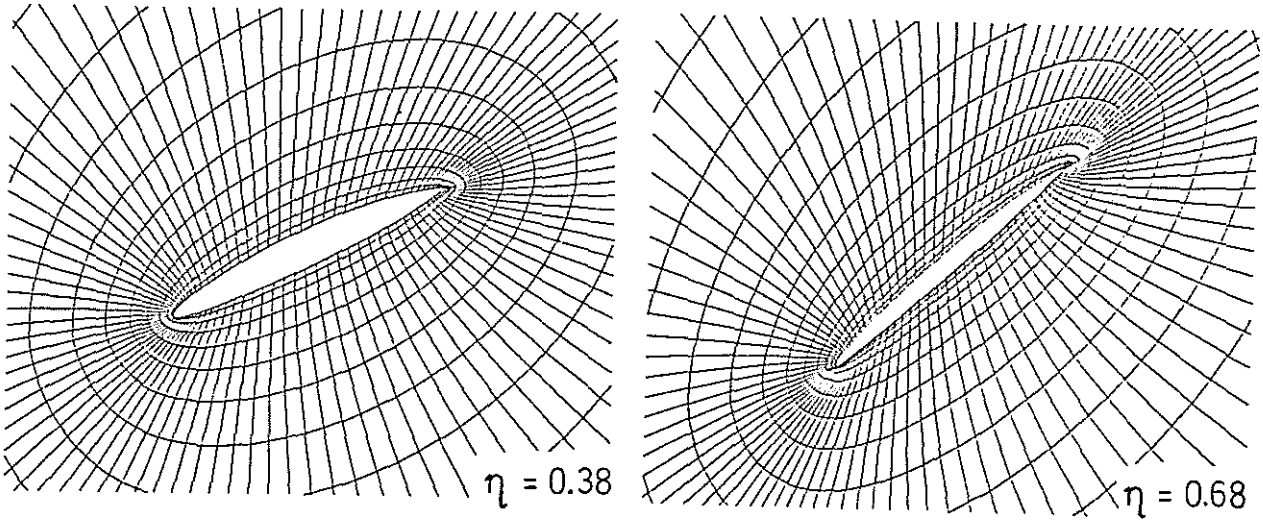

b) Chordwise grid section at 0.38 and 0.68 percent span

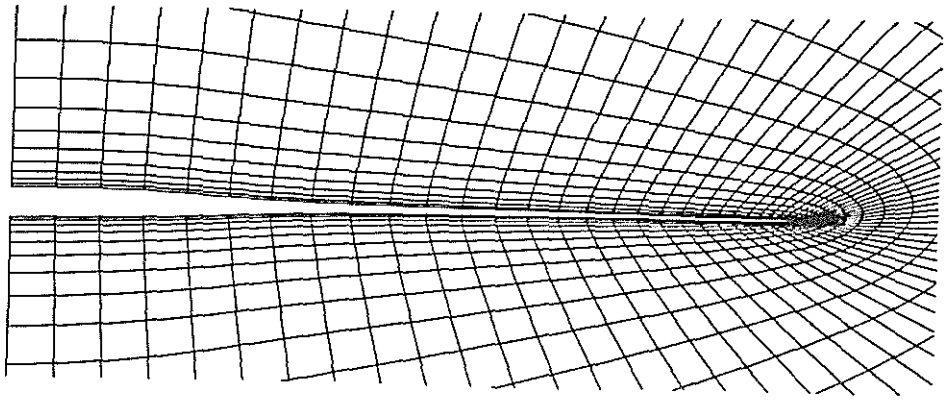

c) Spanwise grid section

Fig. 3 Computational grid around a propeller blade

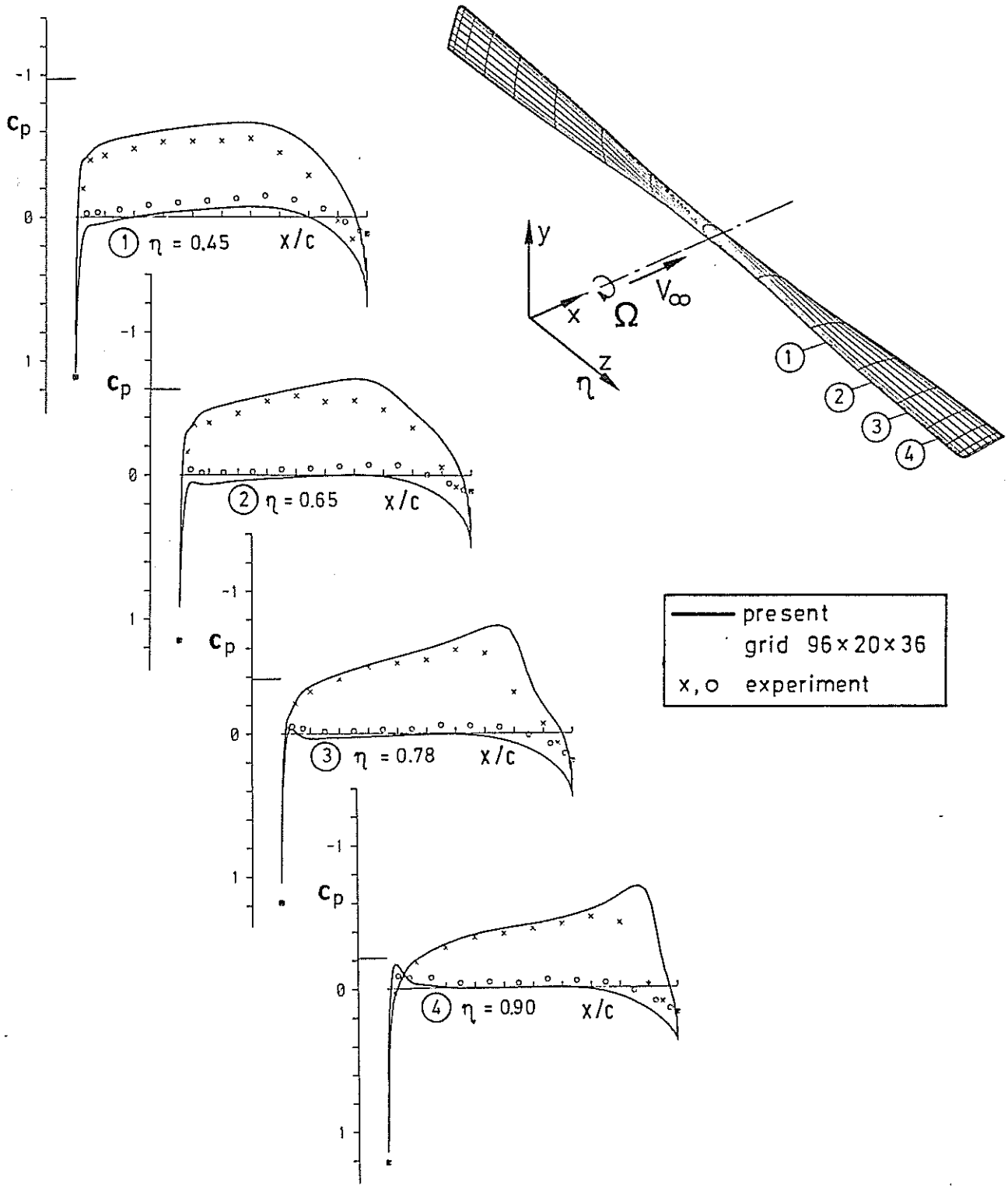

Fig. 4 Chordwise pressure coefficients for the NACA 10-(3)(066)-033 propeller, M_∞ = 0.56 and advance ratio J = 2.3

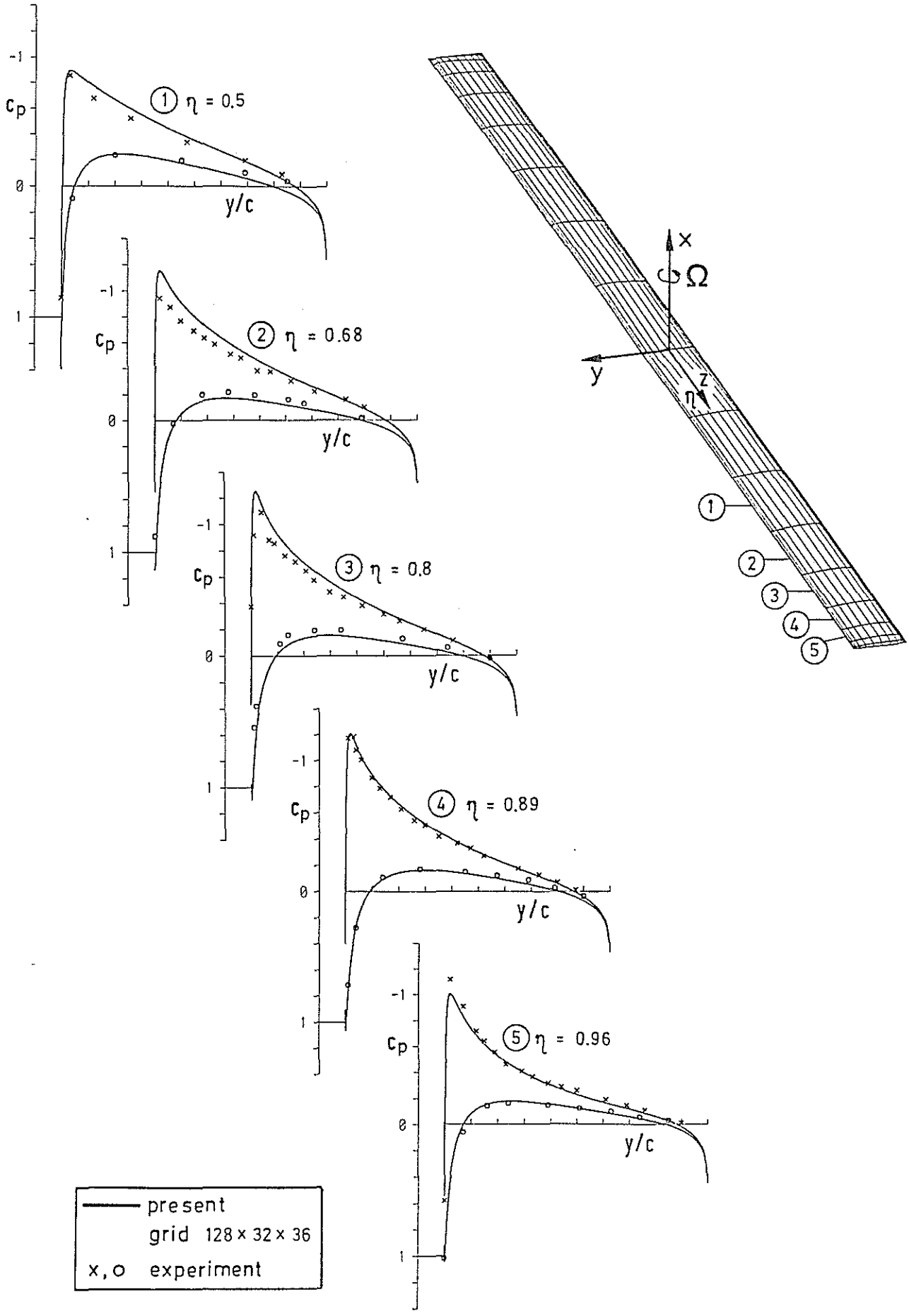

Fig. 5 Chordwise pressure coefficients for the model rotor in hover, $M_{tip} = 0.439$, $\theta = 8^{o}$.

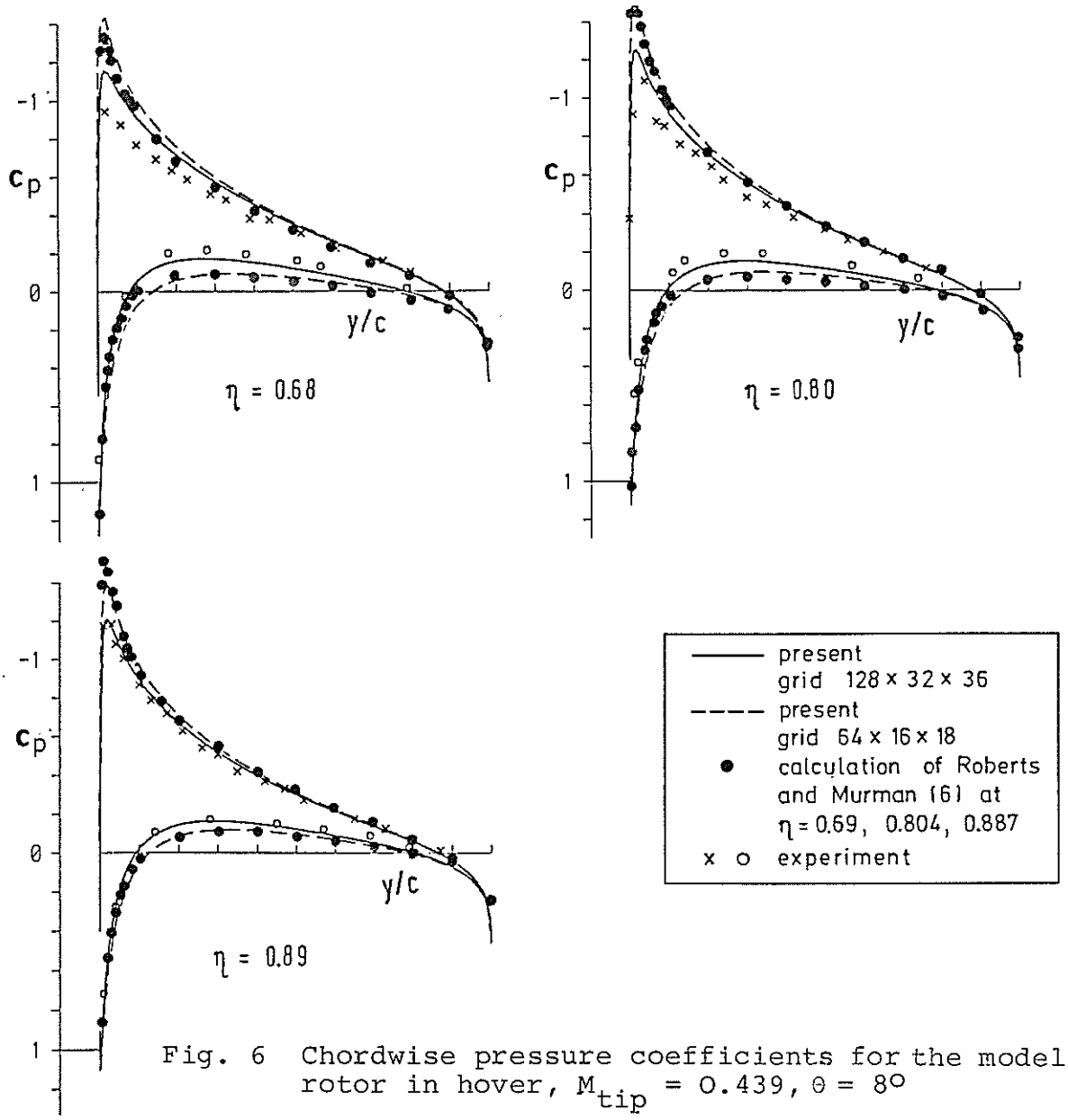

Fig. 6 Chordwise pressure coefficients for the model rotor in hover, $M_{tip} = 0.439$, $\theta = 8^{o}$

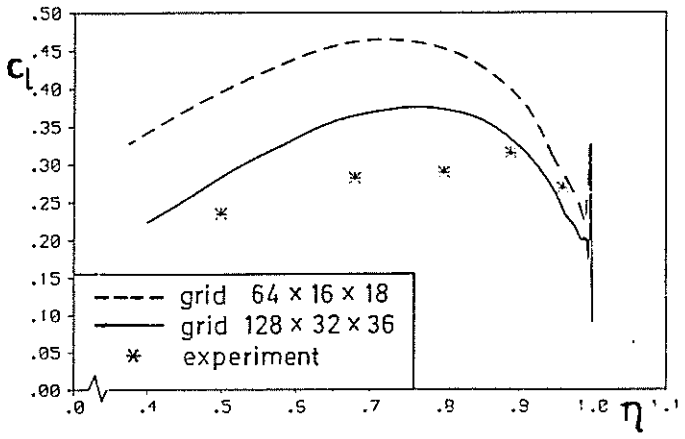

Fig. 7 Spanwise sectional lift coefficients distribution for the model rotor in hover $M_{tip} = 0.439$, $\theta = 8^{o}$

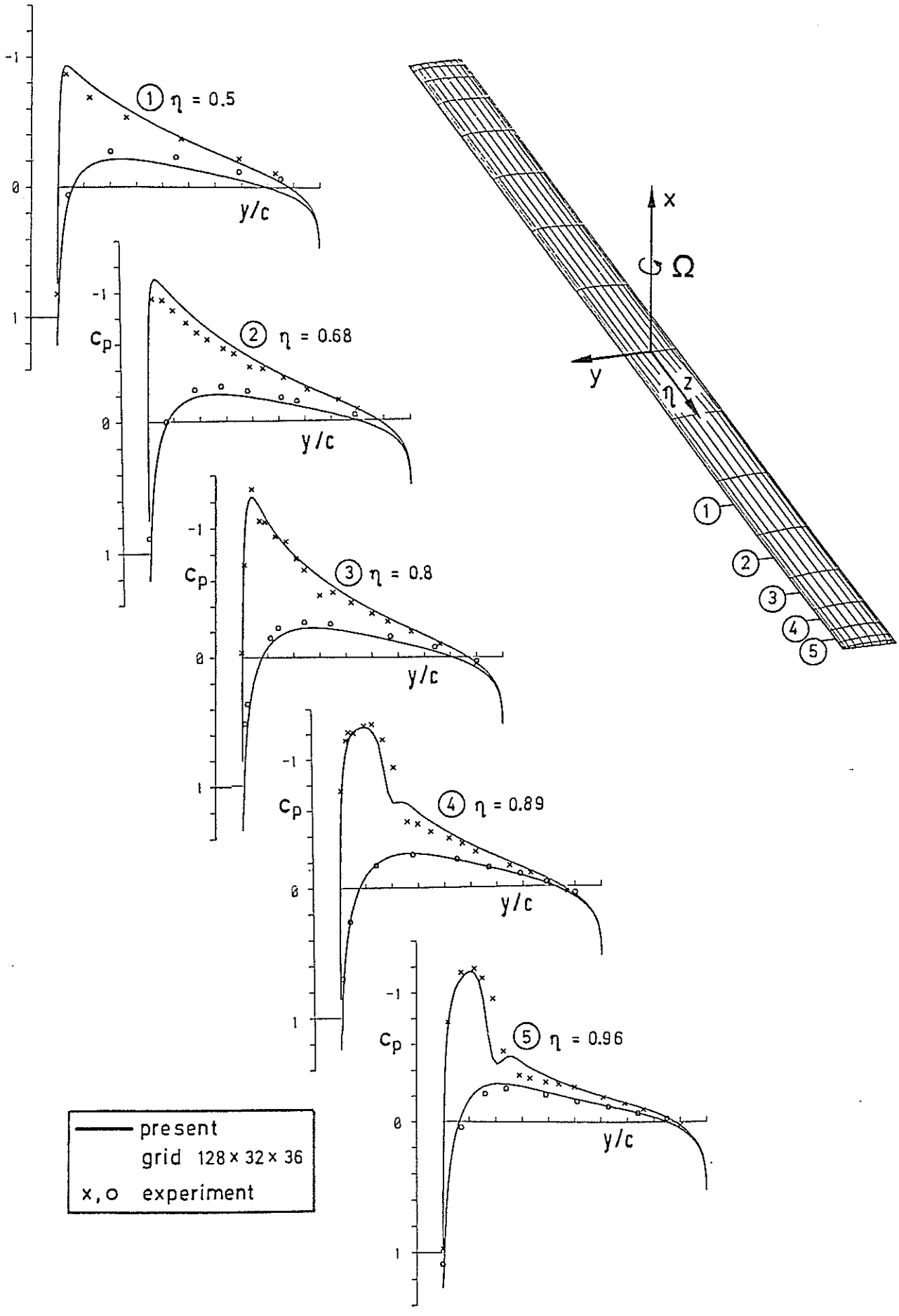

Fig. 8 Chordwise pressure coefficients for the model rotor in hover, $M_{tip} = 0.794$, $\theta = 8^{o}$.